Supporting Information

Small Molecule Donors Based on Benzodithiophene and Diketopyrrolopyrrole Compatible with Both Fullerene and Non-fullerene Acceptors

Yong Huo,[a] Jingshuai Zhu,[c] Xiao-Zhen Wang,[a] Cenqi Yan,[c] Yun-Fei Chai,[a] Zi-Zhen Chen,[a] Xiaowei Zhan*[c] and Hao-Li Zhang*[a,b]

Contents

1 Materials

Unless stated otherwise, all the solvents and chemical reagents were obtained commercially and used without further purification. All reactions dealing with air- or moisture-sensitive compounds were carried out using standard Schlenk techniques. The compound 1[1] and compound 2[2] were synthesized according to the literatures. Compound 6 were purchased from Suna Optoelectronics.

Scheme S1. The synthetic routes of BDTTT-DPP and BDTTVT-DPP.

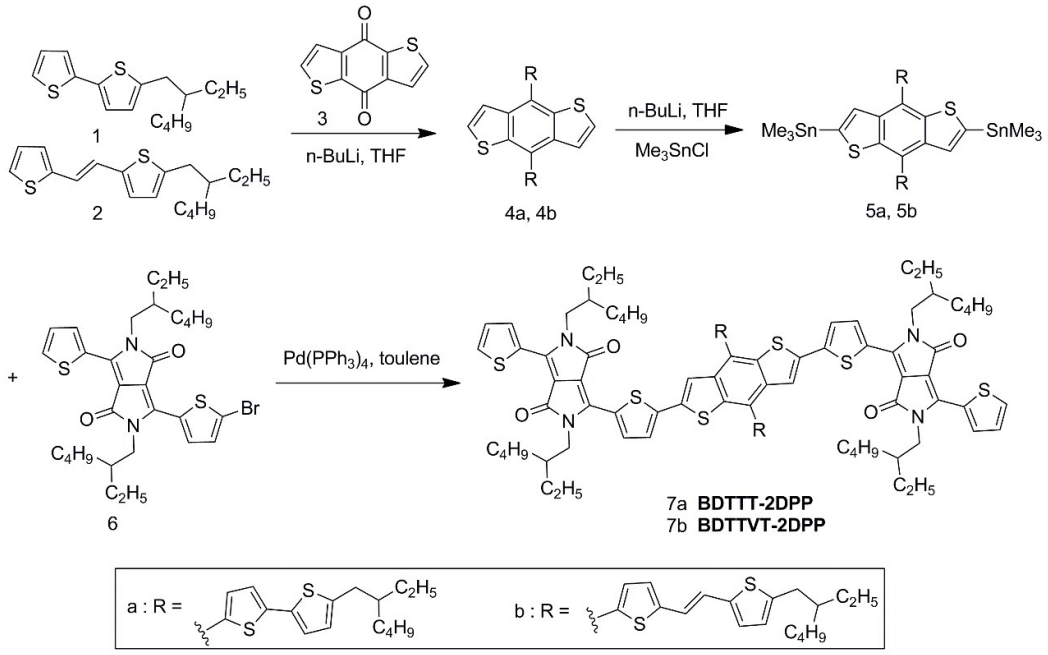

Compound 4a. Under the protection of argon, n-butyllithium (2.4 M, 1.25 mL, 3 mmol) was dropwise added to compound 1 (764 mg, 2.75 mmol) in dry THF (20 mL) at −78 °C over 0.5 h. After being stirred for 0.5 h, the mixture was warmed to room temperature and stirred for another 0.5 h. Benzo[1,2-b:4,5-b']dithiophene-4,8-dione (242 mg, 1.1 mmol) then was quickly added, and the reaction mixture was refluxed at 60 °C for 2 h. The reaction mixture was cooled to room temperature, and a solution of $SnCl_2 \cdot 2H_2O$ (1.0 g, 4.4 mmol) in 10% HCl (10 mL) was added. The reaction mixture was stirred for another 2 h and then poured intoice water. The mixture was

extracted with petroleum ether (20 mL ×2). The organic layer was washed with water and dried over anhydrous Na_2SO_4 for 1 h. After removal of solvent, the crude product was purified by column chromatography on silica gel using petroleum ether as eluent to afford compound 4a as a yellow solid (580 mg, yield = 71%). ^{1}H NMR (400 MHz, $CDCl_3$): δ 7.70(d, J = 5.6 Hz, 2H), 7.48 (d, J = 5.6 Hz, 2H), 7.38 (d, J = 3.6 Hz, 2H), 7.24 (d, J = 3.6 Hz, 2H), 7.08 (d, J = 3.2 Hz, 2H), 6.73 (d, J = 3.2 Hz, 2H), 2.85-2.82 (m, 4H), 1.73 (s, 2H), 1.42-1.32 (m, 18H), 0.93 (m, 12H). ^{13}C NMR (100 MHz, $CDCl_3$): δ 145.83, 139.01, 138.99, 137.65, 136.50, 134.34, 128.81, 127.77, 124.86, 123.67, 123.53, 123.23, 123.11, 31.85, 31.59, 30.19, 29.32, 29.22, 29.07, 22.65, 14.10. MS (MALDI-TOF): *m/z* 743.2 (M^+).

Compound 4b. Under the protection of argon, n-butyllithium (2.4 M, 1.25 mL, 3 mmol) was dropwise added to compound 2 (836 mg, 2.75 mmol) in dry THF (20 mL) at −78 °C over 0.5 h. After being stirred for 0.5 h, the mixture was warmed to room temperature and stirred for another 0.5 h. Benzo[1,2-b:4,5-b']dithiophene-4,8-dione (242 mg, 1.1 mmol) then was quickly added, and the reaction mixture was refluxed at 60 °C for 2 h. The reaction mixture was cooled to room temperature, and a solution of $SnCl_2 \cdot 2H_2O$ (1.0 g, 4.4 mmol) in 10% HCl (10 mL) was added. The reaction mixture was stirred for another 2 h and then poured intoice water. The mixture was extracted with petroleum ether (20 mL ×2). The organic layer was washed with water and dried over anhydrous Na_2SO_4 for 1 h. After removal of solvent, the crude product was purified by silica gel using petroleum ether as eluent to afford compound 4b as a yellow solid (575 mg, yield = 68%). ^{1}H NMR (400 MHz, $CDCl_3$): δ 7.70 (d, J = 5.6

Hz, 2H), 7.49 (d, J = 5.6 Hz, 2H), 7.38 (d, J = 3.6 Hz, 2H), 7.13(d, J = 3.6 Hz, 2H), 7.10-7.06 (d, J = 15.6 Hz, 2H), 7.01-6.97 (d, J = 15.6 Hz, 2H), 6.88 (d, J = 3.6 Hz, 2H), 6.67 (d, J = 3.6 Hz, 2H), 2.76-2.74 (m, 4H), 1.61 (s, 2H), 1.43-1.32 (m, 18H), 0.90 (m, 12H). ^{13}C NMR (100 MHz, $CDCl_3$): δ 144.51, 143.77, 140.05, 138.97, 137.83, 136.49, 128.82, 127.78, 126.45, 125.96, 125.82, 123.78, 123.29, 122.59, 119.87, 41.38, 34.39, 32.39, 29.69, 28.87, 25.54, 22.99, 14.14, 10.84. MS (MALDI-TOF): *m/z* 795.3 (M^+).

Compound 5a. Under the protection of argon, n-butyllithium (2.5 M, 0.5 mL, 1.25 mmol) was dropwise added to compound 4a (372 mg, 0.5 mmol) in dry THF (20 mL) at −78 °C over 0.5 h. After being stirred for 1 h, Me_3SnCl (1 M, 5mL, 5 mmol) was added into the mixture at −78 °C over 0.5 h. The mixture then was warmed to room temperature and stirred for 12 h. Subsequently, the mixture was poured into ice water and extracted with CH_2Cl_2 (20 mL × 2). The organic layer was washed with water and dried over anhydrous Na_2SO_4 for 1 h and concentrated to afford compound 5a, which was used for the next step without purification.

Compound 5b. Under the protection of argon, n-butyllithium (2.5 M, 0.5 mL, 1.25 mmol) was dropwise added to compound 4b (385 mg, 0.5 mmol) in dry THF (20 mL) at −78 °C over 0.5 h. After being stirred for 1 h, Me_3SnCl (1 M, 5 mL, 5 mmol) was added into the mixture at −78 °C over 0.5 h. The mixture then was warmed to room temperature and stirred for 12 h. Subsequently, the mixture was poured into ice water and extracted with CH_2Cl_2 (20 mL × 2). The organic layer was washed with water and dried over anhydrous Na_2SO_4 for 1 h and concentrated to afford compound 5b, which

was used for the next step without purification.

Compound 7a (BDTTT-DPP). A solution of compound 5a (0.5 mmol) and compound 6 (603 mg, 1 mmol) in dry toluene (40 mL) was degassed twice with argon following the addition of $Pd(PPh_3)_4$ (60 mg, 0.05 mmol). After being stirred and refluxed for 24 h at 110 °C with the protection of argon, the reaction mixture was poured into water (100 mL) and extracted with CH_2Cl_2 (100 mL × 2). The organic layer was washed with water twice and dried over anhydrous Na_2SO_4 for 1 h. After removal of solvent, the crude product was purified by silica gel using dichloromethane/petroleum (1:1) as eluant to afford compound 7a as a deep blue solid (697 mg, yield = 78%). ^{1}H NMR (600 MHz, $CDCl_3$)：δ 9.00 (d, J = 4.2 Hz, 2H), 8.91 (d, J = 4.2 Hz, 2H), 7.70 (s, 2H), 7.50 (d, J = 4.8 Hz, 2H), 7.43 (d, J = 3.0 Hz, 2H), 7.32 (d, J = 3.6 Hz, 2H), 7.29 (d, J = 3.0 Hz, 2H), 7.22-7.20 (m, 2H), 7.14 (d, J = 3.6 Hz, 2H), 6.75 (d, J = 3.6 Hz, 2H), 4.03-3.95 (m, 8H), 2.88 (m, 4H), 1.88 (m, 4H), 1.33 (m, 50H), 0.90 (m, 36H). MS (MALDI-TOF): *m/z* 1787.7 (M^+). Anal. calcd for $C_{102}H_{122}N_4O_4S_{10}$: C, 68.49; H, 6.87. Found: C, 68.57; H, 6.94.

Compound 7b (BDTTVT-DPP). A solution of compound 5b (0.5 mmol) and compound 6 (603 mg, 1 mmol) in dry toluene (40 mL) was degassed twice with argon following the addition of $Pd(PPh_3)_4$ (60 mg, 0.05 mmol). After being stirred and refluxed for 24 h at 110 °C with the protection of argon, the reaction mixture was poured into water (100 mL) and extracted with CH_2Cl_2 (100 mL × 2). The organic layer was washed with water twice and dried over anhydrous Na_2SO_4 for 3 h. After removal of solvent, the crude product was purified by silica gel using

dichloromethane/petroleum (1:1) as eluant to afford compound 7b as a deep blue solid (653 mg, yield = 72%). ^{1}H NMR (600 MHz, $CDCl_3$)：δ8.98 (d, J = 4.2 Hz, 2H), 8.91 (d, J = 3.6 Hz, 2H), 7.68 (s, 2H), 7.49 (s, 2H), 7.45 (d, J = 3.0 Hz, 2H), 7.32 (s, 2H), 7.22-7.20 (m, 4H), 7.16-7.13 (d, J = 15.6 Hz, 2H), 7.06-7.02 (d, J = 15.6 Hz, 2H), 6.93 (d, J = 3.0 Hz, 2H), 6.72 (d, J = 2.4 Hz, 2H), 3.99-3.94 (m, 8H), 2.86-2.83 (m, 4H), 1.87 (m, 4H), 1.31 (m, 50H), 0.85 (m, 36H). MS (MALDI-TOF): *m/z* 1839.7 (M^+). Anal. calcd for $C_{106}H_{126}N_4O_4S_{10}$: C, 69.16; H, 6.90. Found: C, 69.30; H, 7.03.

2 Characterization

The ^{1}H NMR and ^{13}C NMR spectra were measured using a Bruker AVANCE 400 MHz spectrometer. Mass spectral data (MS) were obtained with a Bruker esquire6000 mass spectrometer with ESQ6K operator. UV-vis absorption spectra in solution (chloroform) and thin film (on a quartz substrate) used Jasco V-570 spectrophotometer. Elemental analysis was carried out using a Flash EA 1112 elemental analyzer. Electrochemical measurements were carried out under nitrogen in a deoxygenated solution of tetra-*n*-butylammoniumhexafluorophosphate (0.1 M) in acetonitrile using a potential scan rate of 100 mV s^{-1} employing a computer-controlled Zahner IM6e electrochemical workstation. All measurements were carried out at room temperature with a conventional three electrode configuration consisting of a platinum working electrode, a platinum wire auxiliary electrode, and a nonaqueous Ag/AgNO3 reference electrode. Dichloromethane was distilled from calcium hydride under dry nitrogen immediately prior to use. The potentials were referenced to a ferrocenium/ferrocene ($FeCp_2^{+/0}$) couple using ferrocene as an external

standard. Thermogravimetric analysis (TGA) measurements were performed using a Shimadzu thermogravimetric analyzer (Model DTG-60) under flowing nitrogen gas at a heating rate of 10 °C min^{-1}. The nanoscale morphology of the blended films was observed using a Multimode 8 atomic force microscope (Bruker) in the tapping mode. The transmission electron microscopy (TEM) characterization was carried out on JEM-2100 transmision electron microscope operated at 200 kV. The samples for the TEM measurements were prepared as follows: the active-layer films were spin-cast onto ITO/PEDOT:PSS substrates, and the substrates with the active layers were submerged in deionized water to make the active layers float on the air-water interface. Then, the floated films were picked up on unsupported 200 mesh copper grids for the TEM measurements.

Fabrication and characterization of SM-OSCs, NFASM-OSCs and ternary OSCs.

The organic solar cell devices were fabricated and characterized in a N_2-filled glovebox. The device structure was ITO/PEDOT:PSS/active layer/PDIN/Al. Patterned ITO glass (sheet resistance = 15 Ω cm^{-1}) was precleaned in an ultrasonic bath with acetone and isopropanol, and treated in an ultraviolet–ozone chamber (Jelight Company, USA) for 20 min. PEDOT:PSS layer (*ca.* 30 nm) was spin-coated at 4000 rpm onto the ITO glass, and then baked at 150 °C for 15 min. Then donor:acceptor mixture solutions (15 mg mL^{-1} in total for SM-OSCs ,NFASM-OSCs and ternary OSCs) in chloroform were spin-coated (*ca*. 100 nm). Then methanol solution of PDIN at a concentration of 1.0 mg mL^{-1} was spin-coated at 3000 rpm (*ca*. 5 nm) onto the active layer. At last, Al electrode (*ca*. 80 nm) was slowly evaporated

onto the surface of the photoactive layer under vacuum (*ca*. 10^{-5} Pa). The active area of the device was *ca.* 4 mm^2. The *J-V* curve was measured using a computer-controlled B2912A Precision Source/Measure Unit (Agilent Technologies). An XES-70S1 (SAN-EI Electric Co., Ltd.) solar simulator (AAA grade, 70 × 70 mm^2 photobeam size) coupled with AM 1.5 G solar spectrum filters was used as the light source, and the optical power at the sample was 100 mW cm^{-2}. A 2 × 2 cm^2 monocrystalline silicon reference cell (SRC–1000-TC-QZ) was purchased from VLSI Standards Inc. The EQE spectrum was measured using Solar Cell Spectral Response Measurement System QE-R3011 (Enlitech Co., Ltd.). The thickness of organic layer was measured on DektakXT (Bruker).

Mobility measurements

Hole-only or electron-only devices were fabricated using the architectures of ITO/PEDOT: PSS/ active layer/Au for holes and ITO/Al/ active layer /Al for electrons. For hole-only devices, the pre-cleaned ITO glass was spin-coated with PEDOT: PSS (*ca*. 35 nm), then active layers were spin-coated, then Au (*ca*. 30 nm) was evaporated under vacuum (*ca*. 10^{-5} Pa) at a low speed (1 Å/5 s) to avoid the penetration of Au atoms into the active layers. For electron-only devices, Al (*ca*. 80 nm) was evaporated onto pre-cleaned glass under vacuum (*ca*. 10^{-5} Pa), active layers was spin-coated, and then Al (*ca.* 50 nm) was evaporated under vacuum (*ca*. 10^{-5} Pa). The mobility was extracted by fitting the current density–voltage curves using space charge limited current (SCLC). The equation is as follows.

$$J = (9/8)\mu\varepsilon_r\varepsilon_0 V^2 \exp(0.89(V/E_0L)^{0.5})/L^3$$

where J is current density, μ is hole or electron mobility, ε_r is relative dielectric constant, ε_0 is permittivity of free space, $V = V_{appl} - V_{bi}$, E_0 is characteristic field, L is the thickness of organic layer. The J–V curves of the devices are plotted as $\ln[Jd^3/(V_{appl}-V_{bi})^2]$ versus $[(V_{appl}-V_{bi})/d]^{0.5}$.

3 TGA plots of BDTTT-DPP and BDTTVT-DPP

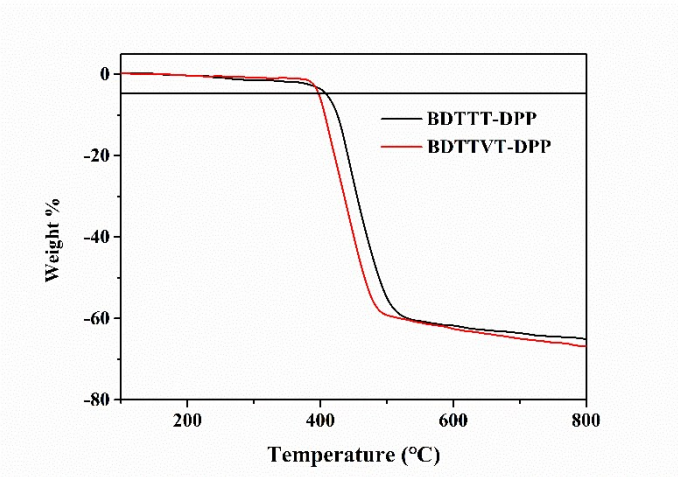

Fig. S1 TGA plot of BDTTT-DPP and BDTTVT-DPP.

4 Cyclic voltammograms of BDTTT-DPP and BDTTVT-DPP

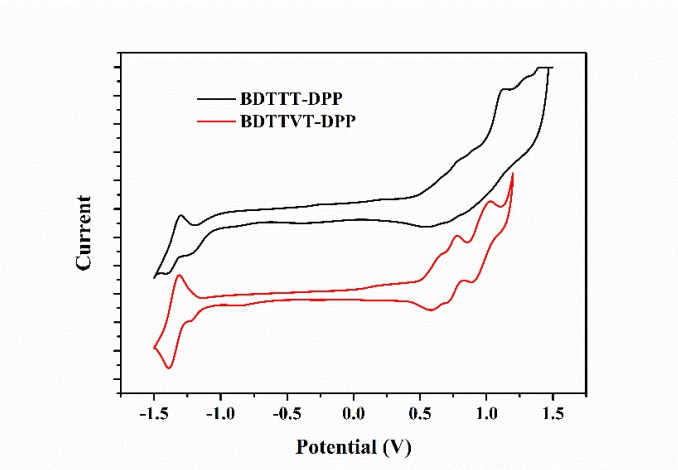

Fig. S2 Cyclic voltammograms of BDTTT-DPP and BDTTVT-DPP in DCM solutions.

5 Hole mobilities of BDTTT-DPP and BDTTVT-DPP film

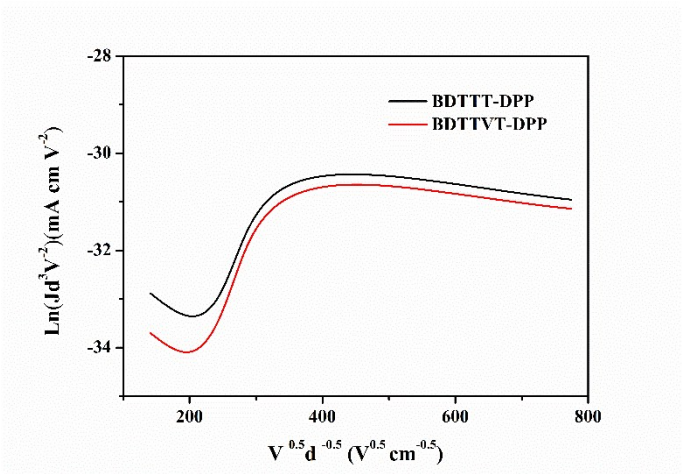

Fig. S3 Hole mobilities of BDTTT-DPP and BDTTVT-DPP.

6 Photoluminescence (PL) quenching tests

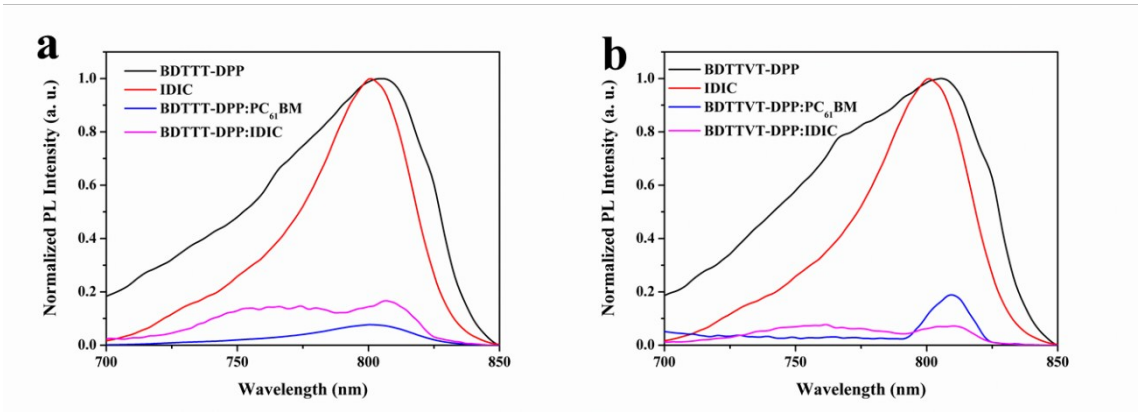

Fig. S4 a) PL quenching between BDTTT-DPP and $PC_{61}BM$/IDIC in the blend film, b) PL quenching between BDTTVT-DPP and $PC_{61}BM$/IDIC in the blend film. Excitation wavelength λ_{Ex} = 640nm. (Note: $PC_{61}BM$ does not show photoluminescence under the given condition).

7 Device optimization for SM-OSCs and NFASM-OSCs

Table S1. Device performance of OSCs with different BDTTT-DPP:$PC_{61}BM$ ratios.

D:A	V_{OC} (V)	J_{SC} (mA cm^{-2})	FF（%）	PCE（%）
1:0.8	0.835	9.63	55.35	4.45
1:1	0.828	10.92	61.05	5.53
1:1.2	0.817	9.16	58.37	4.33

Table S2. Device performance of BDTTT-DPP:$PC_{61}BM$ with different thickness.

thickness	V_{OC} (V)	J_{SC} (mA cm^{-2})	FF（%）	PCE（%）
80	0.823	9.82	62.67	5.06
100	0.828	10.92	61.05	5.53
120	0.830	11.56	50.32	4.82

Table S3. Device performance of OSCs with different BDTTVT-DPP:$PC_{61}BM$ ratios.

D:A	V_{OC} (V)	J_{SC} (mA cm^{-2})	FF（%）	PCE（%）
1:0.8	0.834	7.05	52.67	3.10
1:1	0.830	7.32	57.28	3.48
1:1.2	0.827	7.55	50.65	3.16

Table S4. Device performance of BDTTVT-DPP:$PC_{61}BM$ with different thickness.

thickness	V_{OC} (V)	J_{SC} (mA cm^{-2})	FF（%）	PCE（%）
80	0.827	6.56	60.45	3.28
100	0.830	7.32	57.28	3.48
120	0.833	7.55	51.43	3.23

Table S5. Device performance of OSCs with different BDTTT-DPP:IDIC ratios.

D:A	V_{OC} (V)	J_{SC} (mA cm^{-2})	FF（%）	PCE（%）
1:0.8	0.806	9.68	59.82	4.50
1:1	0.811	10.16	58.28	4.80
1:1.2	0.808	9.56	55.67	4.30

Table S6. Device performance of BDTTT-DPP:IDIC with different blend thickness.

thickness	V_{OC} (V)	J_{SC} (mA cm^{-2})	FF（%）	PCE（%）
60	0.816	9.06	57.67	4.26
80	0.811	10.16	58.28	4.80
100	0.802	9.89	50.67	4.00

Table S7. Device performance of OSCs with different BDTTVT-DPP:IDIC ratios.

D:A	V_{OC} (V)	J_{SC} (mA cm^{-2})	FF%	PCE%

1:0.8	0.825	10.53	51.46	4.47
1:1	0.820	11.30	59.17	5.48
1:1.2	0.818	10.89	54.23	4.83

Table S8. Device performance of BDTTVT-DPP:IDIC with different blend thickness.

thickness	V_{OC} (V)	J_{SC} (mA cm^{-2})	FF（%）	PCE（%）
60	0.811	9.45	58.78	4.50
80	0.820	11.30	59.17	5.48
100	0.823	10.87	51.68	4.62

8 The UV-Vis absorption spectra of BDTTT-DPP:$PC_{61}BM$, BDTTVT-DPP:$PC_{61}BM$, BDTTT-DPP:IDIC and BDTTVT-DPP:IDIC blend films

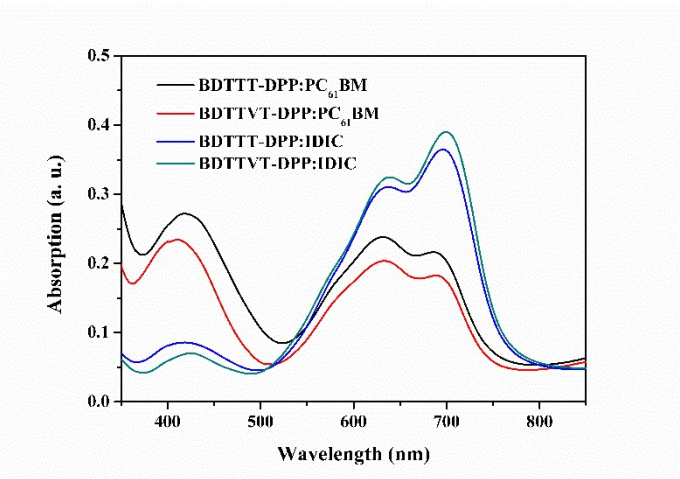

Fig. S5 UV-Vis absorption spectra of the blend films.

9 TEM for as-cast SM-OSCs and NFASM-OSCs

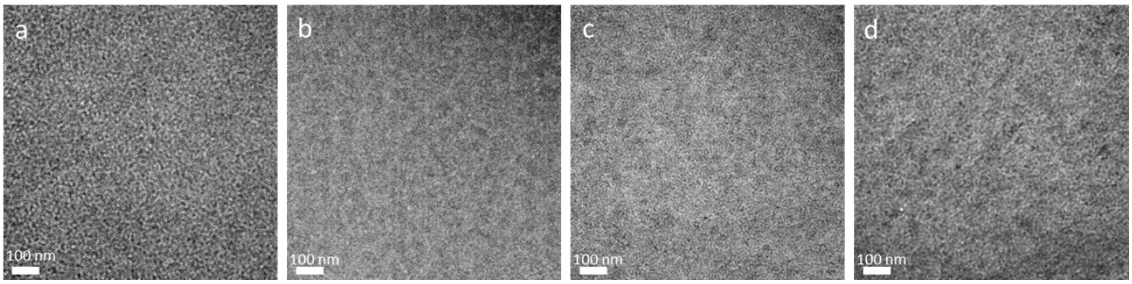

Fig. S6 TEM images of a) BDTTT-DPP:$PC_{61}BM$ film, b) BDTTVT-DPP:$PC_{61}BM$ film, c) BDTTT-DPP:IDIC film and d) BDTTVT-DPP:IDIC film. The scale bars are 100 nm.

10 Hole and electron mobilities test for SM-OSCs and NFASM-OSCs

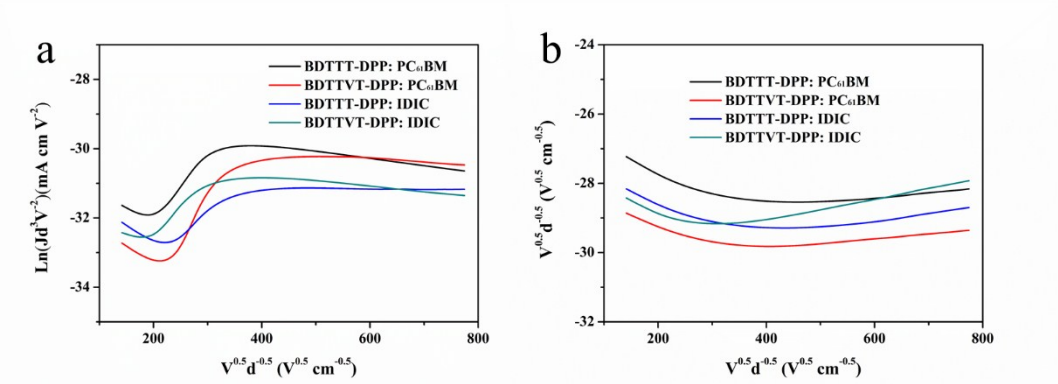

Fig. S7 *J-V* characteristics in the dark for hole-only a) and electron-only b) devices based on BDTTT-DPP:$PC_{61}BM$, BDTTVT-DPP:$PC_{61}BM$, BDTTT-DPP:IDIC and BDTTVT-DPP:IDIC blends.

Table S9. the mobilities of BDTTT-DPP:$PC_{61}BM$, BDTTVT-DPP:$PC_{61}BM$, BDTTT-DPP:IDIC and BDTTVT-DPP:IDIC devices.

Blend	μ_h/cm^{2}V^{-1}s^{-1}	μ_e/cm^{2}V^{-1}s^{-1}	μ_h/μ_e
BDTTT-DPP:$PC_{61}BM$	8.9×10^{-4}	7.4×10^{-4}	1.2
BDTTVT-DPP:$PC_{61}BM$	6.3×10^{-4}	3.1×10^{-4}	2.1
BDTTT-DPP:IDIC	2.0×10^{-4}	3.3×10^{-4}	0.6
BDTTVT-DPP:IDIC	4.7×10^{-4}	4.5×10^{-4}	1.1

11 Ternary device optimization.

Table S10. Ternary device optimization of OSCs with different BDTTT-DPP:IDIC:$PC_{61}BM$ ratios.

D1/IDIC/$PC_{61}BM$	V_{OC} (V)	J_{SC} (mA cm^{-2})	FF (%)	PCE^c (%)	J_{SC}^{cal} (mA cm^{-2})
1:0:1 (100%)	0.83	10.92	61.05	5.53	10.51
1:0.2:0.8(80%)	0.82	10.98	53.72	4.84	10.99
1:0.4:0.6(60%)	0.82	10.51	58.82	5.07	10.34
1:0.6:0.4(40%)	0.82	12.45	63.92	6.53	12.05
1:0.8:0.2(20%)	0.81	11.76	60.38	5.75	11.87
1:1:0(0%)	0.81	10.16	58.28	4.80	9.83

Table S11. Ternary device optimization of OSCs with different BDTTVT-DPP:IDIC:$PC_{61}BM$ ratios.

D1/IDIC/$PC_{61}BM$	V_{OC} (V)	J_{SC} (mA cm^{-2})	FF (%)	PCE[c] (%)	J_{SC}^{cal} (mA cm^{-2})
1:0:1(100%)	0.83	7.32	57.28	3.48	7.14
1:0.2:0.8(80%)	0.83	9.42	55.40	4.33	9.36
1:0.4:0.6(60%)	0.82	9.46	57.95	4.50	9.32
1:0.6:0.4(40%)	0.82	10.54	58.39	5.11	10.23
1:0.8:0.2(20%)	0.82	12.66	63.02	6.55	12.28
1:1:0(0%)	0.82	11.30	59.17	5.48	11.23

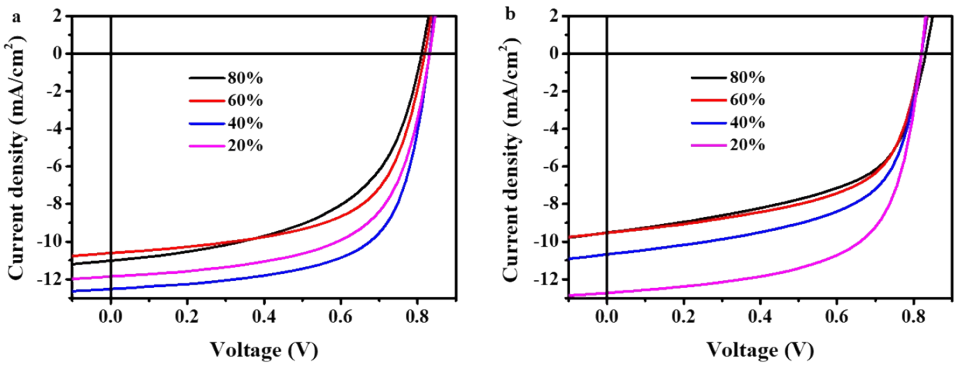

Fig. S8 *J-V* curves for ternary devices of (a) BDTTT-DPP and (b) BDTTVT-DPP.

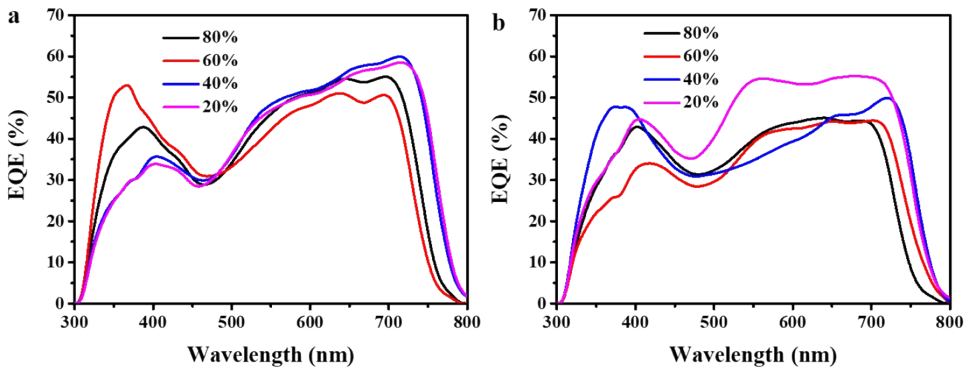

Fig. S9 EQE curves for ternary devices of (a) BDTTT-DPP and (b) BDTTVT-DPP.

12 References

1. Zhou, J.; Zuo, Y.; Wan, X.; Long, G.; Zhang, Q.; Ni, W.; Liu, Y.; Li, Z.; He, G.; Li, C.; Kan, B.; Li, M.; Chen, Y., Solution-processed and high-performance organic solar cells using small molecules with a benzodithiophene unit. *J. Am. Chem. Soc.*, 2013**,** ***135***, 8484-8487.
2. Yao, H.; Zhang, H.; Ye, L.; Zhao, W.; Zhang, S.; Hou, J., Molecular Design and

Application of a Photovoltaic Polymer with Improved Optical Properties and Molecular Energy Levels. *Macromolecules* 2015**,** ***48***, 3493-3499.